Electrical synaptic transmission between fast-spiking interneurons is facilitated by insulin

Satoshi Kosukegawa
Nihon University Graduate School of Dentistry
Major in Orthodontics
(Directors: Profs. Mitsuru Motoyoshi and Masayuki Kobayashi,
and Asst. Prof. Yuka Nakaya)

Index

This thesis is based on the following article and additional results in terms of synergisity evaluation of electrical synapses (Fig. 4):

Satoshi Kosukegawa, Yuka Nakaya, Satomi Kobayashi, Kohei Kitano, Sachie Matsumura, Shohei Ogisawa, Manabu Zama, Mitsuru Motoyoshi, and Masayuki Kobayashi (2023) Insulin facilitates synaptic transmission via gap junctions between fast-spiking interneurons in the rat insular cortex. J Oral Sci, in press.

Abstract

Inhibitory synaptic currents from fast-spiking neurons (FSNs), a typical gamma-aminobutyric acid (GABA)ergic interneuron in the cerebral cortex, to pyramidal neurons are facilitated by insulin. FSNs frequently show electrical synapses to FSNs, however, the effect of insulin on these electrical synapses has been unknown. In this study, electrical synaptic potentials via gap junction between FSNs were recorded to examine how insulin modulates these potentials in the rat insular cortex (IC). Bath application of insulin (10 nM), which increases the spike firing rate of pyramidal neurons and unitary inhibitory postsynaptic currents recorded from FSN to pyramidal neuron connections, slightly but significantly increased electrical synaptic currents. The mean ratio of electrical synapses, the coupling coefficient, that is obtained by postsynaptic voltage responses divided by presynaptic voltage amplitude was 8.3 ± 1.1% in control and 9.2 ± 1.1% during 10 nM insulin application. Input resistance and voltage responses to large hyperpolarizing currents (−140 pA) were not changed by insulin. These results suggest that insulin facilitates spike synchronization by increasing electrical synaptic currents via gap junctions of GABAergic FSNs in the IC.

Introduction

Insulin receptors are highly expressed in the cerebral cortex [1]. Several previous studies have demonstrated the modulation of neural activities by insulin in the cerebral cortex. Insulin increases repetitive spike firing of pyramidal neurons, which is due to the hyperpolarization of the action potential threshold in the insular cortex (IC) [2]. It is worth noting that gamma-aminobutyric acid (GABA)ergic neurogliaform cells, whose repetitive firing pattern is classified as fast-spiking, release insulin in combination with GABA, suggesting that insulin may play a role in GABAergic synaptic transmission in the cerebral cortex [3]. Indeed, inhibitory postsynaptic potentials (IPSPs) recorded from pyramidal neurons are potentiated by insulin [4].

Fast-spiking neurons (FSNs) induce IPSPs not only in pyramidal neurons [5] but also in FSNs themselves [6, 7]. In addition, electrical synapses are frequently observed between FSNs [6, 8]. Therefore, neuronal activities of FSNs are regulated by themselves in addition to excitatory inputs. Interestingly, several neuromodulators have been reported to regulate the coupling coefficient, the efficacy of electrical synaptic transmission, in both peripheral and central nervous systems. Nitric oxide increases cyclic adenosine monophosphate (cAMP) concentration and the coupling coefficient in viscero-parietal peptidergic neurons [9]. Met-enkephalin significantly increased the coupling coefficient between pedal A cluster neurons [10]. In the central nervous system, vasoactive intestinal peptide modulates the coupling coefficient in the suprachiasmatic nucleus [11]. However, no information is available on insulin-dependent modulation of electrical synapses via gap junctions in the cerebral cortex.

The present study aimed to examine the effect of insulin on the coupling coefficient between FSNs in the insular cortex.

Materials and Methods

All experiments were approved by the Institutional Animal Care and Use Committee at the Nihon University (AP21DEN019-3). The present experiments were performed according to the National Institutes of Health Guide for the Care and Use of Laboratory Animals. The present experiments complied with the journal's ethical principles.

Animals and slice preparation

Acute slice preparations were prepared for electrophysiological recording as previously reported using vesicular-GABA transporter (VGAT)-Venus line A transgenic rats [12-15] (either sex; postnatal weeks 3-4). Isoflurane (5%; Pfizer, Tokyo, Japan) was used to anesthetized rats. The brain including the IC was rapidly removed and stored for 3 min in ice-cold, modified artificial cerebrospinal fluid (ACSF), whose composition was 230 sucrose, 2.5 KCl, 10 $MgSO_4$, 1.25 NaH_2PO_4, 26 $NaHCO_3$, 0.5 $CaCl_2$, and 10 D-glucose in mM. Coronal slices (350 μm thickness) were cut using a microslicer (LinearSlicer Pro 7, Dosaka EM, Kyoto, Japan). Slices were incubated at 32°C for 10 min in normal ACSF (pH 7.35-7.40): 126 NaCl, 3 KCl, 2 $MgSO_4$, 1.25 NaH_2PO_4, 26 $NaHCO_3$, 2 $CaCl_2$, and 10 D-glucose in mM. The modified and normal ACSF solutions were continuously aerated with a mixture of 95% O_2/5% CO_2. Slices were incubated at room temperature before recording.

Multiple whole-cell patch-clamp recording

A recording chamber was perfused with normal ACSF (2.4 ml/min). Multiple whole-cell patch-clamp recordings were performed from Venus-positive fluorescent neurons in the IC using a fluorescence microscope equipped with Nomarski optics (BX51, Olympus, Tokyo, Japan) and an infrared-sensitive video camera (Hamamatsu Photonics, Hamamatsu, Japan). The voltage and current signals were recorded by amplifiers (Multiclamp 700B, Molecular Devices, USA), digitized (Digidata 1440A, Molecular Devices), observed online, and stored on a computer hard disk using Clampex (pCLAMP 10, Molecular Devices).

The composition of the pipette solution for recordings was as follows (in mM): 85.4 potassium gluconate, 70 KCl, 10 HEPES, 0.5 EGTA, 2 $MgCl_2$, 2 ATP, and 0.3 GTP. The pipette solution had a pH of 7.3 and an osmolality of 300 mOsm. The liquid junction potential (−9 mV) was not corrected. The estimated reversal potential of Cl^- currents was −15.4 mV. A Flaming-Brown micropipette puller (P-97, Sutter Instruments, USA) was used to make thin-wall borosilicate patch electrodes (3-5 MΩ). Recordings were obtained at room temperature.

The seal resistance was >10 GΩ. Electrical signals were low-pass filtered at 5-10 kHz and digitized at 20 kHz.

The neural subtypes of recorded neurons were examined by application of long (500 ms) hyperpolarizing and depolarizing current pulse injections in addition to examining Venus fluorescence. The interstimulus interval between the train pulses was 15 s. To evaluate the coupling coefficient of the electrical synaptic transmission between neurons, voltage responses to −140 pA current pulses from presynaptic and postsynaptic neurons were measured. Then, the percentage ratio obtained by the voltage deflection of the postsynaptic neurons divided by that of presynaptic neurons was calculated. All recordings were obtained under the current clamp condition. Insulin (10 nM; Sigma–Aldrich, USA) was applied to the perfusate. Unless otherwise specified, chemicals were purchased from Wako Pure Chemical Industries (Osaka, Japan) or Nakalai Tesque (Kyoto, Japan).

Data analysis and statistics

Current and voltage responses were analyzed using Clampfit (pCLAMP 10; Molecular Devices). Voltage responses to hyperpolarized current pulses whose duration was set at 500 ms were quantified by averaging those from 50 ms to 450 ms.

Data are presented as the mean ± standard error of the mean. Origin software (Origin 2021b, OriginLab, USA) was used for the statistical analysis. Comparisons of the voltage response amplitude and the coupling coefficient of electrical synaptic transmission between in control and during insulin application were made by paired *t* test. The validity of paired *t* test was checked by the Kolmogorov-Smirnov test. $P < 0.05$ was considered to indicate statistical significance.

Results

Cell identification

Multiple whole-cell patch-clamp recordings were performed from Venus-positive neurons, which were considered to be GABAergic neurons, in the IC. GABAergic neuronal subtypes were identified by application of depolarizing current pulses to induce voltage responses to the rheobase and repetitive spike firing. Cell types of GABAergic neurons were classified into four groups: FSN, low-threshold spike, late spiking, and regular spiking neurons (RSNs) [16,17].

An example of triple whole-cell recording was shown in Fig. 1. FSNs showed an action potential followed by a large and fast afterhyperpolarization and extremely high repetitive firing frequency without spike adaptation (Fig. 1A and B). On the other hand, another neuron showed a prominent adaptation of spike firing, which was called an RSN (Fig. 1C). Chemical synapses from FSN1 to FSN2 (Fig. 1Aa and b) and from FSN2 to RSN were found (Fig. 1Ba and b). In the present study, E_{Cl}- was set at −15 mV to visualize GABAergic synaptic transmission clearly at the resting membrane potential. Therefore, in response to the repetitive spike firing of the presynaptic neurons, FSN1 in Fig. 1Ab and FSN2 in Fig. 1Bb, postsynaptic neurons, FSN2 in Fig. 1Ab and RSN in Fig. 1Bb, showed synaptic depolarizations.

An electrical synapse was found between FSN1 and FSN2 as shown in Fig. 1Ac and Bc. Responding to the hyperpolarization of the presynaptic neurons, FSN1 in Fig. 1Ac and FSN2 in Fig. 1Bc, postsynaptic neurons, FSN2 in Fig. 1Ac and FSN1 in Fig. 1Bc, showed hyperpolarization. It should be noted that the depolarization of postsynaptic neuronal response shown in FSN2 of Fig. 1Ab and FSN1 of Fig. 1Bb involved both chemical and electrical synaptic potentials. In addition, as previously reported [6], electrical synaptic transmission showed a frequency-dependent coupling coefficient of transmission as shown in Fig. 1Bb FSN1; presynaptic spikes (FSN2) were less efficiently conducted to the postsynaptic neuron (FSN1) than voltage deflection with slow kinetics.

Although Venus-positive neurons involve FSNs and other types of GABAergic neurons, only FSNs were analyzed from the following experiments. This is because electrical synapses were frequently found between FSNs.

Bidirectional electrical synaptic transmission

Electrical synapses among FSNs were invariably bidirectional in the IC as shown in Fig. 2. In this study, 53 FSNs were recorded (7 pentadruple, 4 quadruple, and 1 dual recordings; in sum,

95 pairs) were involved and 14 electrical synapses were detected (14/190; 7.4%).

Rectification of the voltage responses

Voltage responses of FSNs to hyperpolarized current pulse injection were examined to explore the rectification of the responses that are often observed in pyramidal neurons.

Fig. 3A shows a typical example of voltage responses of an FSN (FSN1) to hyperpolarized current pulse injection and those of electrically coupled FSN (FSN2). The voltage deflection gap responding to −130 to −160 pA current pulses looks narrower than that responding to 0 to −30 pA current pulses (Fig. 3B). This tendency was also observed in the responses of the electrically coupled neurons (Fig. 3C).

Synergisity evaluation of electrical synapses

Coupling coefficients of bidirectional electrical synaptic transmission were compared (Fig. 4). The rate that was obtained by the division of the larger coupling coefficient of synaptic transmission was estimated by the smaller: the rate was 1.29 ± 0.11 (n = 6).

Effects of insulin on electrical synapses

Insulin effectively increases the firing frequency of pyramidal neurons [2] and potentiates IPSCs from FSNs to pyramidal neurons in the IC (unpublished observation) has been demonstrated. To evaluate the effect of insulin on the coupling coefficient of electrical synaptic transmission among FSN, large hyperpolarizing current pulses (−140 pA) were applied to presynaptic FSNs and postsynaptic voltage deflections were measured (Fig. 1A). Insulin was applied at the concentration of 10 nM because the previous study revealed that EC50 of insulin on IPSCs is 1.6 nM (unpublished observation).

At first, whether insulin affects the presynaptic voltage responses was examined (Fig. 5A and B). The amplitude of voltage responses to current pulses of −140 pA was not changed by insulin: −29.1 ± 2.3 pA in control and −28.8 ± 1.7 pA during insulin application (n = 12; P = 0.74, paired t test). On the other hand, the coupling coefficient of electrical synaptic transmission (see Materials and Methods) was slightly but significantly increased by insulin: 8.3 ± 1.1 in control and 9.2 ± 1.1 during insulin application (n = 14; P = 0.02, paired t test; Fig. 5C). The normality of distribution of the amplitude of voltage responses to current pulses of −140 pA and the coupling coefficient of electrical synaptic transmission was tested by Kolmogorov-Smirnov test (P = 0.15-0.91).

Discussion

The present study demonstrated that insulin slightly but significantly increased the coupling coefficient between FSNs in the IC. IC did not change the voltage responses to the large (−140 pA) hyperpolarizing current pulses.

Insulin activates tyrosin kinase and its downstream cascades, which include the Src homology 2 domain-containing lipid kinase, PI3-K, and MAPK [18, 19] by phosphorylating intracellular insulin receptor substrate proteins [20]. In the pyramidal neurons of the IC, insulin application increases spike firing by lowering the action potential threshold, which is blocked by wortmannin, a PI3-K inhibitor, or deguelin, a PKB/Akt inhibitor, but not by PD98059, a MAPK inhibitor [2]. On the other hand, previous studies demonstrated that nitric oxide [9], met-enkephalin [10], and vasoactive intestinal peptide [11] play a role in the modulation of the coupling coefficient between neurons. However, these modulators are coupled to various G proteins including G_s, G_q, and $G_{i/o}$, and therefore intracellular transduction pathways are widely varied. In light of these findings, the mechanisms of the insulin-dependent enhancement of the coupling coefficient should be further explored in the future.

As previously demonstrated, electrical synapses between GABAergic interneurons contribute to the synchronization of spike firing [6, 21]. Adopting these findings to this study, such synchronized activities of FSNs may induce potent inhibition in pyramidal neurons in the IC. This looks to contradict the insulin-induced facilitation of spike induction in pyramidal neurons [2]. These findings might make the excitation-inhibition contrast clear: weak excitatory inputs would be diminished by insulin whereas strong excitatory inputs would still elicit action potentials in the pyramidal neurons.

The IC receives visceral information mediated via the vagal nerve [22]. It has been reported that the IC has dense mutual connections between the hypothalamus [23]. One of the principal functions of the hypothalamus is the regulation of feeding behaviors a part of which is controlled by glucose concentration in the blood. The concentration of insulin in the blood increases after feeding, and simultaneously, it is likely that the IC neuronal activities increase by gastric expansion. Insulin in the blood enters the brain via the blood-brain barrier via a saturable transport system [24]. Therefore, the present finding may suggest a functional aspect of insulin in feeding behaviors.

References

1. Schulingkamp RJ, Pagano TC, Hung D, Raffa RB (2000) Insulin receptors and insulin action in the brain: review and clinical implications. Neurosci Biobehav Rev 24, 855-872.

2. Takei H, Fujita S, Shirakawa T, Koshikawa N, Kobayashi M (2010) Insulin facilitates repetitive spike firing in rat insular cortex via phosphoinositide 3-kinase but not mitogen activated protein kinase cascade. Neuroscience 170, 1199-1208.

3. Molnar G, Farago N, Kocsis AK, Rozsa M, Lovas S, Boldog E et al. (2014) GABAergic neurogliaform cells represent local sources of insulin in the cerebral cortex. J Neurosci 34, 1133-1137.

4. Lo FS, Erzurumlu RS (2018) Insulin receptor sensitization restores neocortical excitation/inhibition balance in a mouse model of autism. Mol Autism 9, 13.

5. Kubota Y, Kawaguchi Y (2000) Dependence of GABAergic synaptic areas on the interneuron type and target size. J Neurosci 20, 375-386.

6. Galarreta M, Hestrin S (1999) A network of fast-spiking cells in the neocortex connected by electrical synapses. Nature 402, 72-75.

7. Galarreta M, Hestrin S (2002) Electrical and chemical synapses among parvalbumin fast-spiking GABAergic interneurons in adult mouse neocortex. Proc Natl Acad Sci USA 99, 12438-12443.

8. Galarreta M, Hestrin S (2001) Electrical synapses between GABA-releasing interneurons. Nat Rev Neurosci 2, 425-433.

9. Sidorov AV, Kazakevich VB, Moroz LL (1999) Nitric oxide selectively enhances cAMP levels and electrical coupling between identified RPaD2/VD1 neurons in the CNS of Lymnaea stagnalis (L.). Acta Biol Hung 50, 229-233.

10. Qazzaz MM, Winlow W (1999) Effect of volatile anaesthetics on the electrical activity and the coupling coefficient of weakly electrically coupled neurones. Acta Biol Hung 50, 199-213.

11. Wang MH, Chen N, Wang JH (2014) The coupling features of electrical synapses modulate neuronal synchrony in hypothalamic superachiasmatic nucleus. Brain Res 1550, 9-17.

12. Uematsu M, Hirai Y, Karube F, Ebihara S, Kato M, Abe K et al. (2008) Quantitative chemical composition of cortical GABAergic neurons revealed in transgenic venus-expressing rats. Cereb Cortex 18, 315-330.

13. Murayama S, Yamamoto K, Kaneko M, Ogiso B, Kobayashi M (2017) Ablation of C-fibers decreases quantal size of GABAergic synaptic transmission in the insular cortex. Neuroscience 365, 179-191.

14. Takei H, Yamamoto K, Bae YC, Shirakawa T, Kobayashi M (2017) Histamine H_3 heteroreceptors suppress glutamatergic and GABAergic synaptic transmission in the rat insular cortex. Front Neural Circuits 11, 85.

15. Yamamoto K, Kobayashi M (2018) Opposite roles in short-term plasticity for N-Type and P/Q-Type voltage-dependent calcium channels in GABAergic neuronal connections in the rat cerebral cortex. J Neurosci 38, 9814-9828.

16. Kawaguchi Y, Kubota Y (1997) GABAergic cell subtypes and their synaptic connections in rat frontal cortex. Cereb Cortex 7, 476-486.

17. Koyanagi Y, Yamamoto K, Oi Y, Koshikawa N, Kobayashi M (2010) Presynaptic interneuron subtype- and age-dependent modulation of GABAergic synaptic transmission by β-adrenoceptors in rat insular cortex. J Neurophysiol 103, 2876-2888.

18. Plum L, Schubert M, Brüning JC (2005) The role of insulin receptor signaling in the brain. Trends Endocrinol Metab 16, 59-65.

19. van der Heide LP, Ramakers GMJ, Smidt MP (2006) Insulin signaling in the central nervous system: learning to survive. Prog Neurobiol 79, 205-221.

20. White MF (1997) The insulin signalling system and the IRS proteins. Diabetologia 40, S2-17.

21. Gibson JR, Beierlein M, Connors BW (1999) Two networks of electrically coupled inhibitory neurons in neocortex. Nature 402, 75-79.

22. Cechetto DF, Saper CB (1987) Evidence for a viscerotopic sensory representation in the cortex and thalamus in the rat. J Comp Neurol 262, 27-45.

23. Allen GV, Saper CB, Hurley KM, Cechetto DF (1991) Organization of visceral and limbic connections in the insular cortex of the rat. J Comp Neurol 311, 1-16.

24. Rhea EM, Rask-Madsen C, Banks WA (2018) Insulin transport across the blood-brain barrier can occur independently of the insulin receptor. J Physiol 596, 4753-4765.

Figures

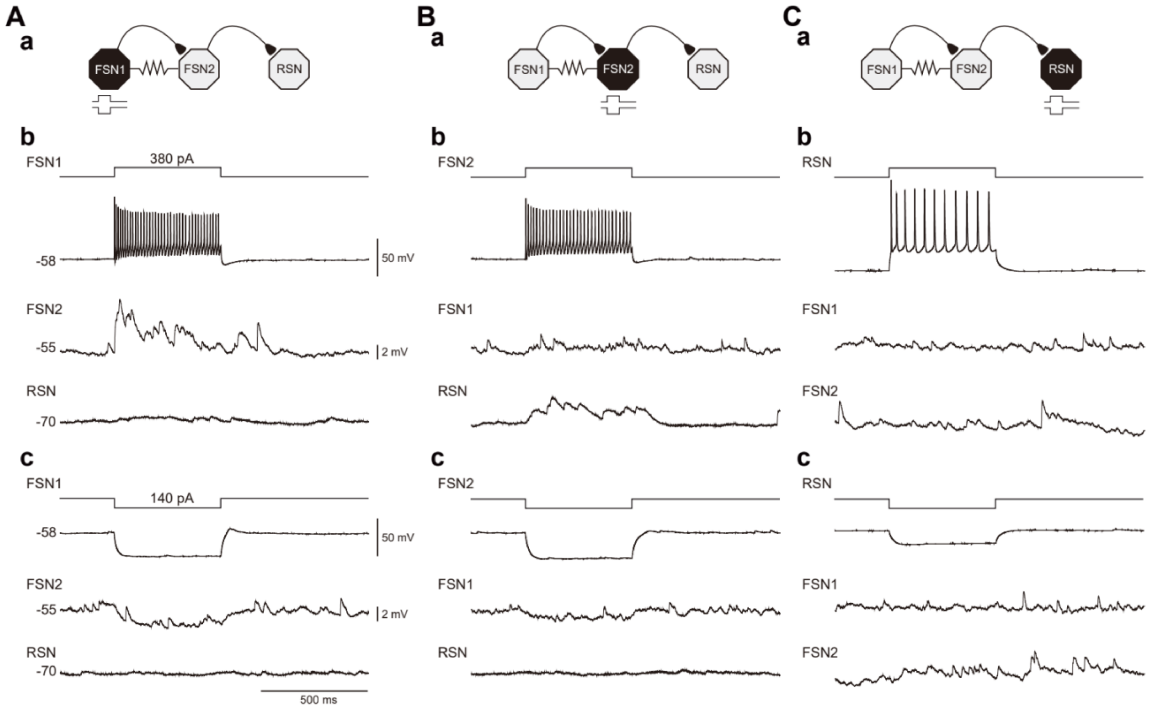

Figure 1. An example of triple whole-cell patch-clamp recording from GABAergic neurons, i.e. fast-spiking neurons (FSN1 and FSN2), and a regular spiking neuron (RSN). ***A.*** Depolarizing (380 pA) and hyperpolarizing current (−140 pA) pulse injection into FSN1 (***a***), which showed high-frequency repetitive spike firing with less spike adaptation. Responding to spike firing of FSN1, FSN2 but not RSN showed synaptic responses (***b***). Hyperpolarizing current pulse injection to FSN1 induced hyperpolarization in FSN2 but not in RSN (***c***). ***B.*** Depolarizing and hyperpolarizing current pulse injection into FSN2 (***a***), which showed high-frequency repetitive spike firing with less spike adaptation. Responding to spike firing of FSN2, RSN showed synaptic responses (***b***). Small spikes in FSN1 responding to spike firing of FSN2 reflect voltage responses via the gap junction between FSN1 and FSN2. Hyperpolarizing current pulse injection to FSN2 induced hyperpolarization in FSN1 but not in RSN (***c***). ***C.*** Depolarizing and hyperpolarizing current pulse injection into RSN (***a***), which showed low-frequency repetitive spike firing with spike adaptation. Neither spike firing nor hyperpolarizing current pulses of RSNs did not induce any synaptic responses in both FSN1 and FSN2 (***b, c***).

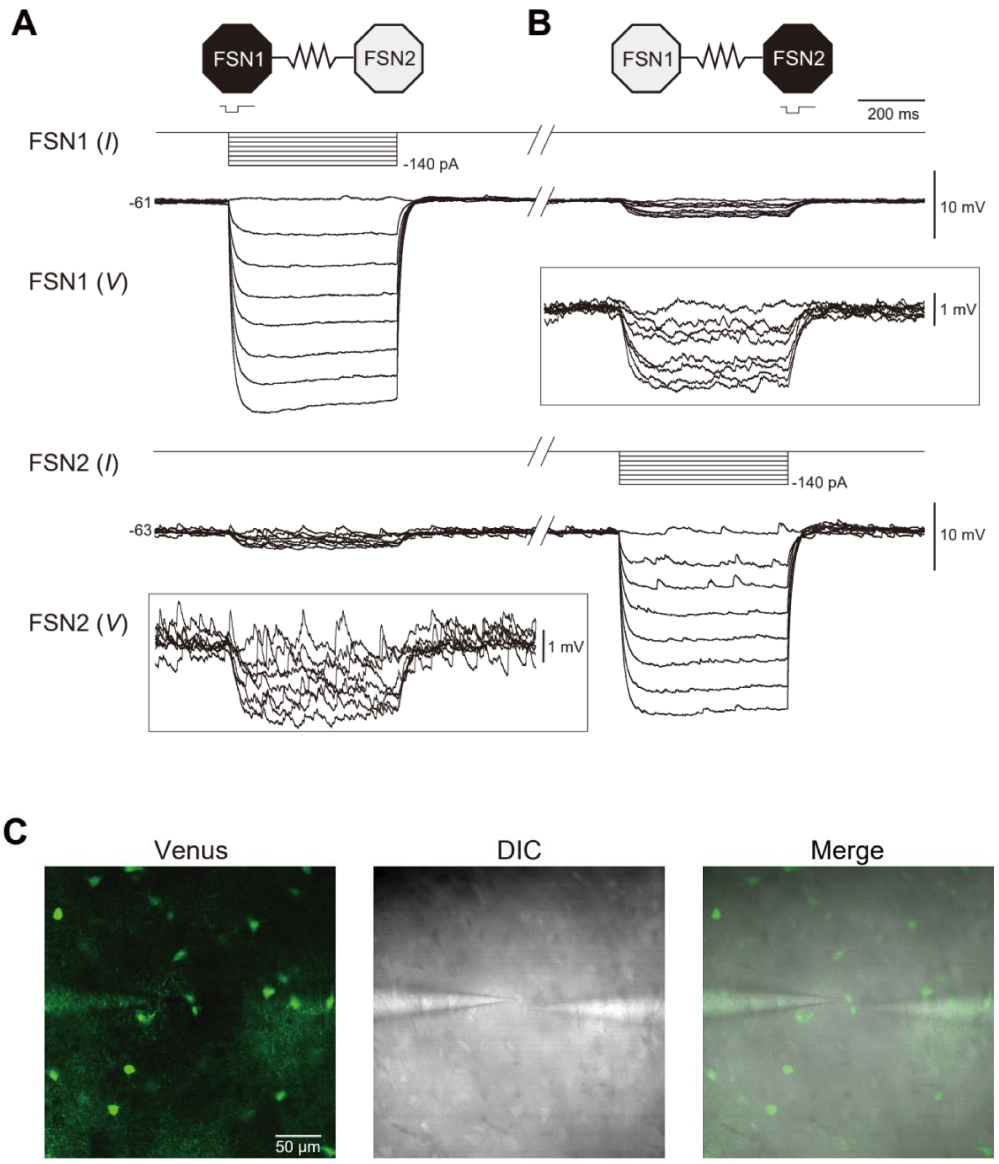

Figure 2. Reciprocal electrical synaptic transmission between FSNs. ***A.*** An example of paired whole-cell patch-clamp recording from two FSNs that are coupled with electrical but not chemical synapses. Hyperpolarizing current pulse injection [(FSN1 (*I*)] into FSN1 induced large voltage responses in FSN1 as shown in FSN1 (*V*), and small voltage responses in FSN2 as shown in FSN2 (*V*). The traces in the rectangular indicates voltage-expanded traces of FSN2 (*V*). ***B.*** The voltage responses in FSN1 and FSN2 to hyperpolarizing current pulse injection into FSN2. ***C.*** The Venus fluorescence and differential interference contrast (DIC) images of recorded neurons shown in A and B.

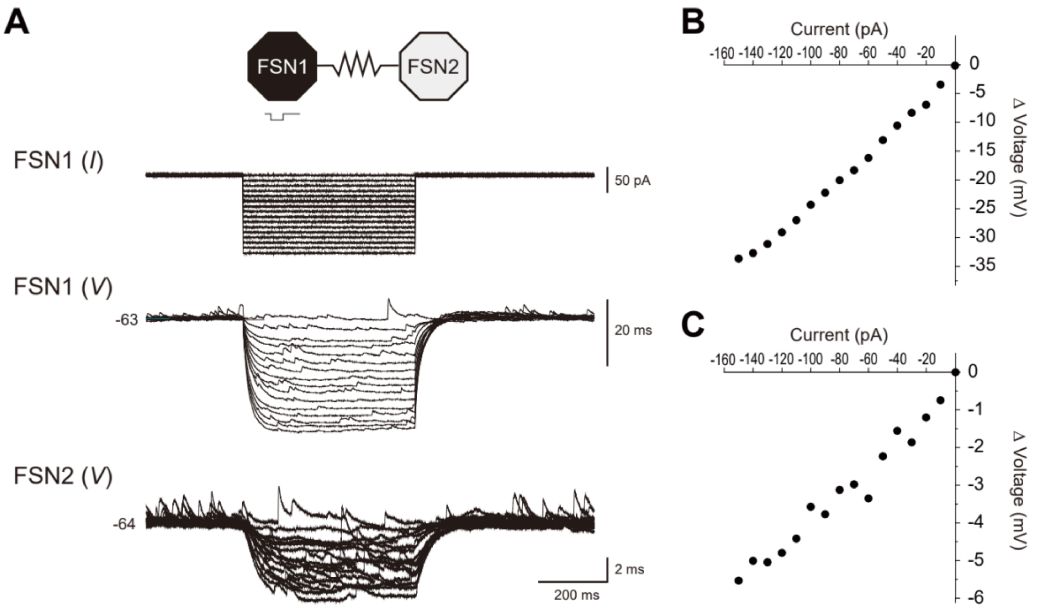

Figure 3. Rectification of voltage responses to hyperpolarizing current pulses in FSNs. ***A.*** An example of voltage responses in an electrically coupled FSN pair. Negative current pulse injection to FSN1, FNS1(*I*), hyperpolarized membrane potential in both FSN1, FSN1 (*V*), and FSN2, FSN2 (*V*). ***B.*** *V*/*I* curve obtained from the FSN1 in (***A***). ***C.*** *V*/*I* curve obtained from the FSN2 in (***A***).

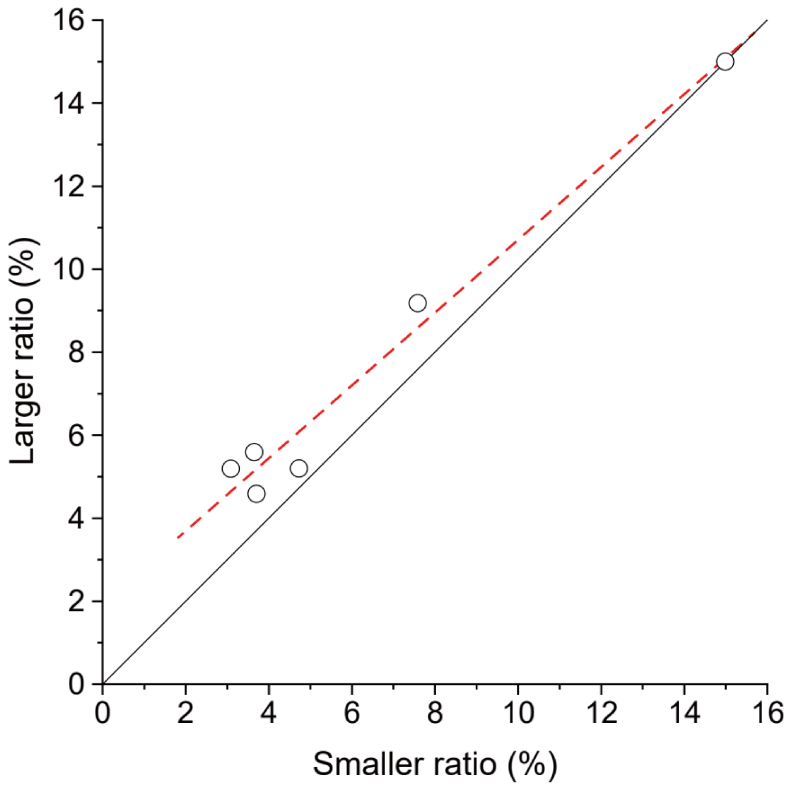

Figure 4. Evaluation of electrical synapse synergisity between FSNs. The percentage ratio obtained by the voltage deflection of the postsynaptic neurons divided by that of presynaptic neurons responding to −140 pA current pulses. Smaller and larger coupling coefficients are plotted on the X- and Y-axis, respectively.

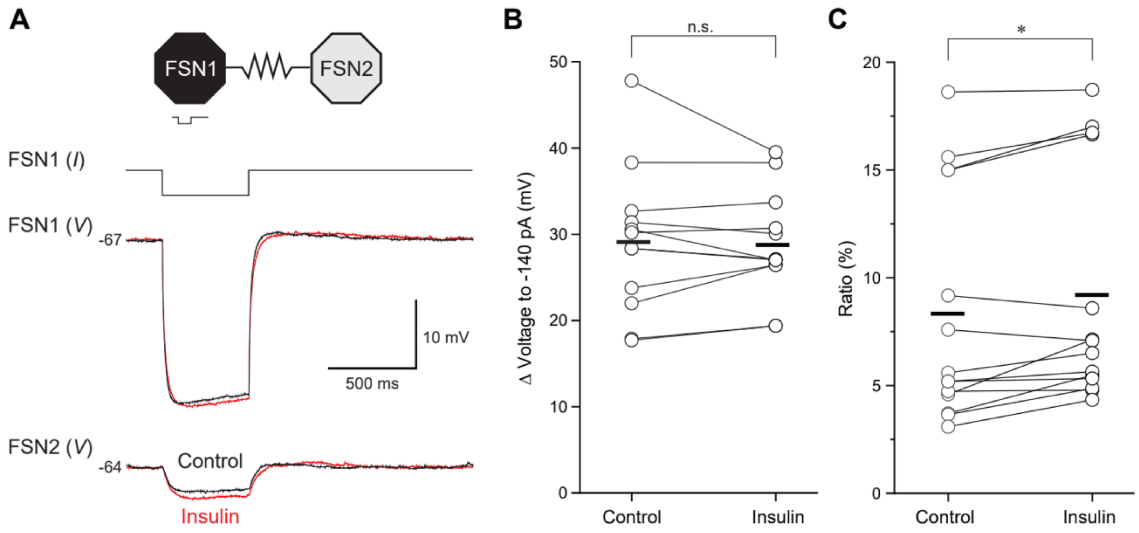

Figure 5. The effect of insulin on electrical synapses between FSNs. ***A.*** An example of voltage responses in an electrically coupled FSN pair, FSN1 and FSN2. Negative current pulse injection to FSN1 hyperpolarized membrane potential in both FSN1 and FSN2, FSN2 (*V*). Bath application of insulin (10 nM) had little effect on the voltage responses in FSN1 but increased those in FSN2. ***B.*** Voltage responses obtained from presynaptic FSNs, which received −140 pA current pulses, in control and during 10 nM insulin application ($n = 12$). ***C.*** The percentage ratio obtained by the voltage deflection of the postsynaptic neurons divided by that of presynaptic neurons responding to −140 pA current pulses in control and during 10 nM insulin application ($n = 14$). Thick horizontal lines indicate the average. n.s.: not significant, *: $P < 0.05$, paired *t* test.